Cell

The Replication Checkpoint Protects Fork Stability by Releasing Transcribed Genes from Nuclear Pores

Rodrigo Bermejo,[1,8,*] Thelma Capra,[1,8] Rachel Jossen,[1,8] Arianna Colosio,[1] Camilla Frattini,[1] Walter Carotenuto,[1] Andrea Cocito,[1] Ylli Doksani,[1,2] Hannah Klein,[3] Belén Gómez-González,[4] Andrés Aguilera,[4] Yuki Katou,[5] Katsuhiko Shirahige,[6] and Marco Foiani[1,7,*]

[1]Fondazione Istituto FIRC di Oncologia Molecolare (IFOM) at IFOM-IEO Campus, Via Adamello 16, 20139 Milan, Italy
[2]Rockefeller University, New York, NY 10065, USA
[3]New York University School of Medicine, New York, NY 10016, USA
[4]Centro Andaluz de Biología Molecular y Medicina Regenerativa CABIMER, Universidad de Sevilla, 41004 Seville, Spain
[5]Tokyo Institute of Technology, 226-8503 Yokohama City, Japan
[6]Research Center for Epigenetic Disease, Institute of Molecular and Cellular Biosciences, Tokyo University, Bunkyo-ku, 108-8639 Tokyo, Japan
[7]DSBB-Università degli Studi di Milano, 20139 Milan, Italy
[8]These authors contributed equally to this work
*Correspondence: rodrigo.bermejo@ifom-ieo-campus.it (R.B.), marco.foiani@ifom-ieo-campus.it (M.F.)
DOI 10.1016/j.cell.2011.06.033

SUMMARY

Transcription hinders replication fork progression and stability, and the Mec1/ATR checkpoint protects fork integrity. Examining checkpoint-dependent mechanisms controlling fork stability, we find that fork reversal and dormant origin firing due to checkpoint defects are rescued in checkpoint mutants lacking THO, TREX-2, or inner-basket nucleoporins. Gene gating tethers transcribed genes to the nuclear periphery and is counteracted by checkpoint kinases through phosphorylation of nucleoporins such as Mlp1. Checkpoint mutants fail to detach transcribed genes from nuclear pores, thus generating topological impediments for incoming forks. Releasing this topological complexity by introducing a double-strand break between a fork and a transcribed unit prevents fork collapse. Mlp1 mutants mimicking constitutive checkpoint-dependent phosphorylation also alleviate checkpoint defects. We propose that the checkpoint assists fork progression and stability at transcribed genes by phosphorylating key nucleoporins and counteracting gene gating, thus neutralizing the topological tension generated at nuclear pore gated genes.

INTRODUCTION

ATR/Mec1 and ATM/Tel1 stabilize stalled (Lopes et al., 2001) and terminal replication forks (Doksani et al., 2009), preventing their collapse (Branzei and Foiani, 2010) and accumulation of recombinogenic X-shaped reversed forks (Doksani et al., 2009; Sogo et al., 2002). Reversed forks are processed by the Exo1 nuclease (Cotta-Ramusino et al., 2005; Lopes et al., 2001) into gapped structures (Sogo et al., 2002). Checkpoint mutants experiencing replication stress fail to resume fork progression (Branzei and Foiani, 2010; Segurado and Diffley, 2008) and fire additional replicons (Santocanale and Diffley, 1998; Shirahige et al., 1998).

Hydroxyurea (HU) causes dNTP depletion, inhibiting replicative polymerases. Consequently, replication forks stall and accumulate short RPA-ssDNA stretches (Sogo et al., 2002; Zou and Elledge, 2003) that trigger Mec1 activation. Mec1 then activates the Rad53 kinase, which protects stalled fork stability through mechanisms that are still obscure.

DNA topology influences fork reversion. In vitro, reversed forks accumulate at positively supercoiled plasmids upon replisome dissociation (Postow et al., 2001b). The thermodynamic energy accumulated as torsional stress in front of replication forks causes fork reversal characterized by parental strands reannealing and nascent strands extrusion and pairing (Postow et al., 2001a; Schvartzman and Stasiak, 2004). Our current knowledge of the in vivo architectural organization of replicating chromosomes is limited. It has been predicted that those sites anchoring chromosomes to membranes behave as topological barriers, preventing the rotation of the DNA helix strands around each other and thus impeding the diffusion of topological changes (Postow et al., 2004; Wang, 2002). In principle, topological barriers might arise at sites where transcribed genes associate to fixed nuclear envelope structures. In eukaryotes, messenger RNA (mRNA) synthesis is coupled with mRNA processing, mRNP (messenger ribonucleoparticle) assembly, and export to the cytoplasm (Aguilera, 2005; Köhler and Hurt, 2007). These processes are coordinated by protein complexes tethering transcribed chromatin to the nuclear pore complex (NPC). THO is

a complex, composed of Tho2, Hpr1, Mft1 and Thp2, that travels with the RNA polymerase II (Luna et al., 2008). THO also associates with Yra1 and Sub2 (to form the TREX complex) and factors involved in mRNA export, including the TREX-2 (or THSC) complex. TREX-2 is constituted by Sac3, Thp1, Sus1, and Cdc31 proteins (Köhler and Hurt, 2007). Sac3 interacts with Cdc31 and Sus1 (Jani et al., 2009) and mediates the association of the complex to the nuclear envelope by binding to the Nup1 nucleoporin at the NPC inner basket. Mutants in THO and TREX-2 genes share transcriptional elongation defects, transcription-associated hyperrecombination (TAR), and mRNA export defects (Luna et al., 2008). THO and TREX-2 are also required for the association of transcribed genes to the NPC (Cabal et al., 2006; Drubin et al., 2006; Rougemaille et al., 2008). This process, known as gene gating, assists rapid gene expression coupling mRNA transcription and export to the cytoplasm and has been implicated in a myosin-like Mlp1-dependent transcriptional memory mechanism (Tan-Wong et al., 2009).

The THO-TREX-2-mediated physical association of the transcribed DNA with the NPC might hinder DNA strand rotation establishing topological barriers. Transcribed genes represent the most abundant sites of replication fork pausing in the yeast genome, and replisome pausing at transcribed genes is independent of the polarity between replication and transcription (Azvolinsky et al., 2009). The mechanisms causing replication/transcription interference may not simply reflect the clash between forks and transcriptional machineries, as the Rrm3 helicase, which facilitates fork progression by removing protein obstacles, does not act at highly transcribed genes (Azvolinsky et al., 2009). Moreover, DNA topoisomerase II (Top2) seems to modulate DNA topology at sites of replication/transcription interference (Bermejo et al., 2009).

We found that mutations in THO and TREX-2 genes counteract HU sensitivity and fork reversal in checkpoint mutants, thus sustaining replication fork progression. Rad53 releases transcribed genes from the nuclear envelope in response to replication stress. Several nucleoporins, including Mlp1, are phosphorylated by checkpoint kinases (Smolka et al., 2005, 2007). *mlp1* mutants mimicking constitutive phosphorylation by Rad53 rescue *rad53* HU sensitivity. Disrupting the tethering of transcribed genes to the NPC or introducing a double-strand break (DSB) between a fork and a highly transcribed gene alleviates the HU sensitivity and counteracts fork reversal in checkpoint-defective cells. We propose that the Mec1/ATR and Rad53-dependent replication checkpoint promotes replication fork stability by controlling gene gating, thus counteracting topological stress-driven fork reversal.

RESULTS

Identification of *rad53* Suppressors

rad53-K227A mutants (Zheng et al., 1993), in 0.2 M HU, accumulate reversed forks and hemireplicated intermediates that can be visualized by electron microscopy and two-dimensional (2D) gels (Lopes et al., 2001; Sogo et al., 2002). Reversed forks migrate on 2D gels as a cone signal characterized by cruciform intermediates spanning from fully duplicated molecules to structures of lower mass, resulting from Exo1-dependent resection (Cotta-Ramusino et al., 2005; Lopes et al., 2001). At lower HU concentrations, Exo1 does not significantly contribute to reversed fork processing and *rad53-K227A* cells accumulate unresected X spikes (data not shown).

Two nonmutually exclusive hypotheses predict that fork reversal results from topological transitions such as accumulation of positive supercoiling (Postow et al., 2001b) and/or runoff of hemicatenane structures likely representing precatenane derivatives (Bermejo et al., 2008; Cotta-Ramusino et al., 2005).

We designed genetic screens aimed at identifying factors influencing *rad53-K227A* viability at low HU doses. We used the yeast deletion library (Tong et al., 2001), searching for those gene deletions rescuing the HU sensitivity caused by overexpression of the dominant-negative *rad53-D339A* mutation (Fay et al., 1997). The suppressors, validated in the W303 genetic background (Thomas and Rothstein, 1989), were also able to rescue the *rad53-K227A* mutation. Deletions of *SAC3*, *THO2 HPR1*, *THP2*, *MFT1*, *SUS1*, and *THP1* (Figure S1 available online) suppressed *rad53* and *mec1* HU sensitivity (Figures 1A–1C and data not shown). THO and TREX2 mutations per se do not counteract the inhibitory effects caused by HU because the single-deletion mutants are sensitive to high HU concentrations and are synthetic sick in combination with *rad53* (data not shown; Gómez-González et al., 2009). Transcriptome analyses showed that *SAC3* ablation did not significantly affect the expression of the Rad53-dependent damage-inducible genes in wild-type or *rad53* cells (data not shown). TREX-2 and THO mutations do not accelerate S phase progression at low HU concentrations, as would be the case for mutants exhibiting elevated dNTP levels (data not shown). Although THO/TREX-2 mutants exhibit mild transcriptional defects (Gómez-González et al., 2011), we cannot rule out that the *rad53* suppression mechanism is, in part, due to reduced transcriptional obstructions to replication.

TREX-2 and THO Mutations Rescue *rad53* Fork Defects

TREX-2 and THO mutations cause recombinogenic events ascribed to R loops (González-Aguilera et al., 2008; Huertas and Aguilera, 2003). In vitro and in vivo observations indicate that nascent mRNAs can prime DNA synthesis (Pomerantz and O'Donnell, 2008, 2010). We investigated whether the ability of TREX-2-THO mutations to rescue *rad53* defects was due to repriming of DNA synthesis downstream of collapsed forks by engaging trapped mRNAs at R loops. This would imply that the mechanism of suppression would be influenced by RNase H overexpression, as in the case of R loop accumulation and transcriptional and recombination abnormalities in THO mutants (Huertas and Aguilera, 2003). *RNH1* (RNase H1) overexpression or ablation of endogenous RNase H1 (*RNH1*) or RNase H2 subunits (*RNH201*, *RNH202*) did not influence the HU sensitivity of *rad53* or *sac3 rad53* cells (Figures 2A and 2B). Hence, the suppression of TREX-2-THO mutations does not depend on the aberrant accumulation of R loops.

We then analyzed the effect of *SAC3* ablation on *rad53* replicon dynamics (Figure 3A) by immunoprecipitation of BrdU-substituted DNA followed by high-density oligo array hybridization (BrdU-IP-Chip) (Fachinetti et al., 2010). At low doses of HU, wild-type forks emanating from early replication origins

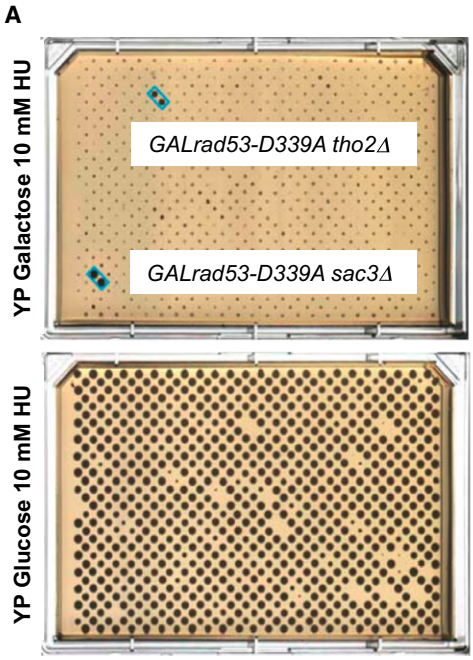

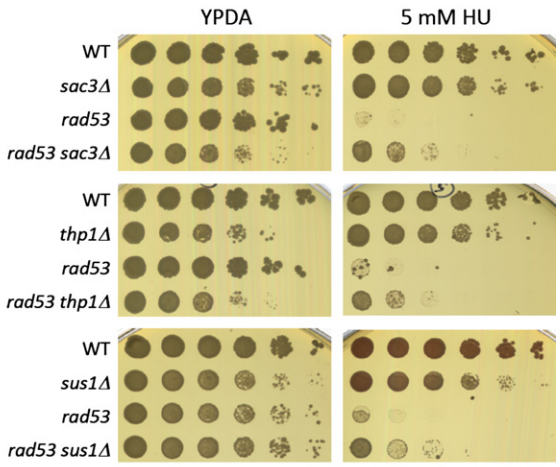

C

	Gene	Human ortholog	Null	*rad53* rescue	ss with *rad53*	HU sensitivity	Phosphosites
THO							
	HPR1	THOC1	viable	+	+	+	S675 (Mec1/Tel1)
	THP2		viable	+	+	+	
	THO2	THOC2	viable	+	+	+	
	MFT1		viable	+	+	+	
TREX							
	TEX1		viable	nd	nd	nd	
	YRA1	THOC4	lethal	nd	nd	nd	
	SUB2	BAT1	lethal	nd	nd	nd	
TREX-2							
	SAC3	SHD1 GANP	viable	+	+	+	
	CDC31		lethal	nd	nd	nd	
	SUS1	ENY2	viable	+	-/+	+	
	THP1	Q5JVF3	viable	+	+	+	
NPC inner basket							
	NUP1		viable	+	-/+	-	S637 (Rad53)
	NUP2		viable	-	-	+	S317 (Rad53)
	NUP60	NUP153	viable	-	-	-	S480 (Rad53)
	MLP1	TPR	viable	+	-	-/+	S1710 (Rad53) S1223, S1670 (Dun1) S2034, S2050 (ATR)
NPC							
	NSP1	NUP62	lethal	nd	nd	nd	S361 (Rad53)
	NUP133	NUP133	viable	-	-	+	

Figure 1. TREX-2 and THO Ablations Rescue *rad53* HU Sensitivity

(A) *GAL-rad53-D339A* SGA YP galactose or YP glucose plates containing 10 mM HU. White boxes mark suppressors of *rad53-D339A* HU sensitivity.

(B) WT, *sac3Δ*, *rad53-K227A*, *rad53-K227A sac3Δ*, *thp1Δ*, *rad53-K227A thp1Δ*, *sus1Δ*, and *rad53-K227A sus1Δ* cells plated without (YPDA) or with 5 mM HU.

(C) Summary of THO/TREX, TREX-2, and NPC genes and their genetic interactions with *rad53-K227A*. Human orthologs are indicated. Null, gene deletion phenotype; *rad53* rescue, suppression of *rad53-K227A* lethality at 5–10 mM HU; *ss* with *rad53*, synthetic sickness in combination with *rad53-K227A*; HU sensitivity, growth defects at 100–200 mM HU; phosphosites, the residues targeted by the checkpoint kinases (in parentheses) are shown.

For schematic summary, see Figure S1.

progressed slowly (Lopes et al., 2001), generating BrdU tracks spanning several kilobases outward of the origin sequences (Figure 3A). In *rad53* cells, shorter BrdU tracks around early origins were observed due to fork collapse and consequent failure to incorporate BrdU (Feng et al., 2006; Lopes et al., 2001; Sogo et al., 2002). Concomitantly, additional BrdU tracks appeared at late/dormant origins (Santocanale and Diffley, 1998; Shirahige et al., 1998). Though *SAC3* ablation per se did not cause

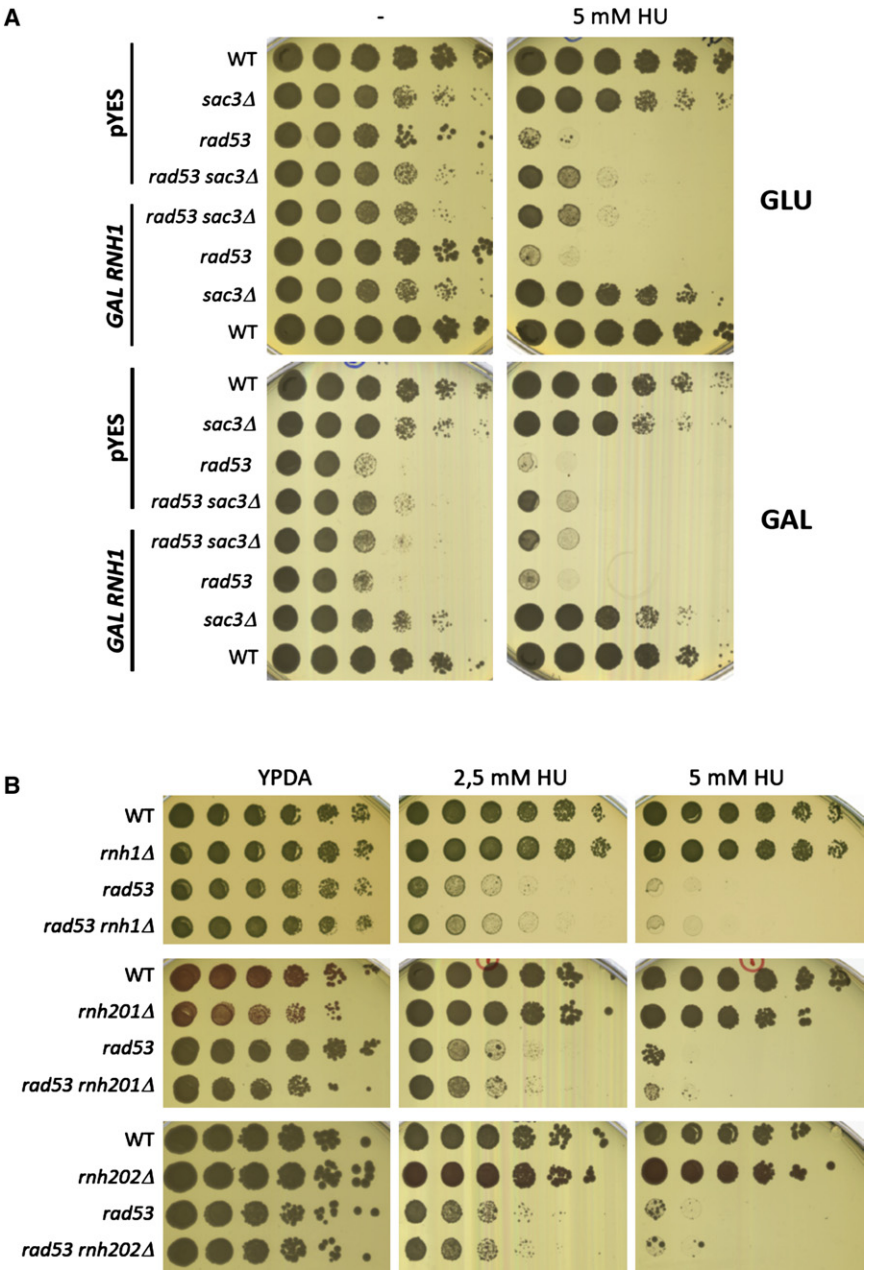

Figure 2. RNase H Overexpression Does Not Influence *rad53* or *rad53 sac3* Cells' HU Sensitivity

(A) WT, *sac3Δ*, *rad53-K227A*, and *rad53-K227A sac3Δ* cells carrying either the vector (pYES) or pGW-RNH1, expressing *RNH1* under the *GAL1* promoter (*GAL RNH1*), were plated in glucose (GLU)- or galactose (GAL)-containing media without (–) or with 5 mM HU.

(B) WT, *rnh1Δ*, *rad53-K227A*, *rad53-K227A rnh1Δ*, *rnh201Δ*, *rad53-K227A rnh201Δ*, *rnh202Δ*, and *rad53-K227A rnh202Δ* cells were plated without (YPDA) or with 2.5 or 5 mM HU.

significant changes in replicon dynamics, in *rad53*, it rescued both the short BrdU tracks at early origins and the BrdU incorporation at late/dormant origins. Because *SAC3* deletion restores replicon progression at early origins without exhibiting additional origin-unrelated BrdU peaks, we conclude that Sac3 ablation somewhat stabilizes genome-wide *rad53* forks. This further argues against reinitiation events mediated by R loops. The finding that, in *rad53 sac3* cells, stabilization of early replicons correlates with the lack of firing of late/dormant replicons suggests that the two phenomena are mechanistically linked, at least in this genetic background. Because Sac3 plays a global and detrimental role on the progression of HU-challenged forks in *rad53* cells, we tested whether Sac3 affected the accumulation of aberrant replication intermediates in *rad53* mutants. Replication intermediates from wild-type, *sac3*, *rad53*, and *rad53 sac3* strains treated with 25 mM HU were visualized by 2D gels (Figure 3B) at the early origin *ARS305* (Newlon et al., 1993; Poloumienko et al., 2001). Wild-type and *sac3* cells exhibited comparable 2D profiles and accumulated bubbles, which result from origin firing, and large Ys, which arise due to asymmetric fork progression outside of the restriction fragment analyzed (Brewer and Fangman, 1987). At 60–90 min, *rad53* cells accumulated X-shaped intermediates corresponding to unprocessed reversed forks (Cotta-Ramusino et al., 2005; Lopes et al., 2001). Reversed forks detection was reduced in *sac3 rad53* double mutants (Figure 3B).

Hence, *SAC3* ablation rescues replicon dynamics and fork reversal in *rad53* mutants, suggesting that the TREX-2 complex, and by extension THO, may act in coordination with replication forks or even be an integral part of the moving replisome. However, the Hpr1 ChIP-chip genomic clusters did not colocalize with DNA polymerases at active replication origins in HU-treated cells but overlapped throughout the cell cycle with RNA Pol II clusters (Bermejo et al., 2009; Gómez-González et al., 2011). This is consistent with a global role for Hpr1 in transcription elongation and mRNP biogenesis. We note that the Hpr1-binding sites also correlate with Top2 and Hmo1 clusters that represent nonpolar pausing elements for incoming forks (Azvolinsky et al., 2009; Bermejo et al., 2009).

Rad53 Influences Gene Gating

It is reasonable to think that the TREX-2-THO-mediated physical continuity between transcribed chromatin and the nuclear envelope would establish nonpolar barriers preventing the diffusion

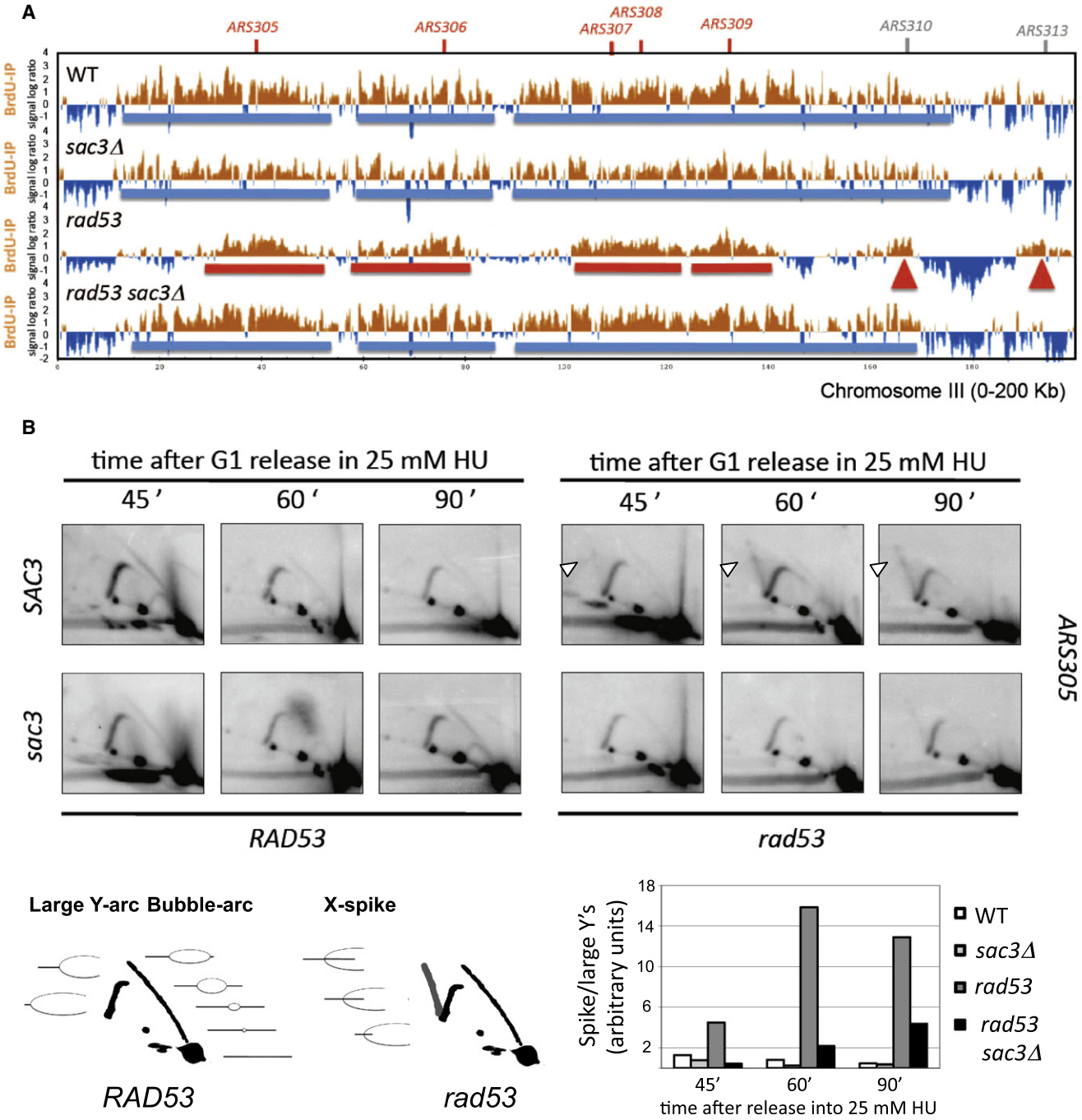

Figure 3. *SAC3* Deletion Suppresses *rad53* Cells' Fork Defects

(A) BrdU-IP-Chip analysis of replicon dynamics of WT, *sac3Δ*, *rad53-K227A*, and *rad53-K227A sac3Δ* cells 60 min after release from G1 into S phase in 25 mM HU. Orange (*BrdU-IP*) histogram bars in the y axis show the average signal ratio in log2 scale of loci along the reported region on chromosome III. The x axis shows chromosomal coordinates. Positions of early and late/dormant *ARS* elements are in red and gray, respectively. Blue and red horizontal bars mark the BrdU incorporation tracks corresponding to forks emanated from early replication origins in WT, *sac3Δ*, and *rad53-K227A sac3Δ* cells or *rad53-K227A* mutants, respectively. Red triangles mark additional BrdU tracks generated by unscheduled dormant origin firing in *rad53-K227A* cells.

(B) 2D gel analysis of replication intermediates in WT (*SAC3 RAD53*), *sac3Δ* (*sac3 RAD53*), *rad53-K227A* (*SAC3 rad53*), and *rad53-K227A sac3Δ* (*sac3 rad53*) cells at the indicated times after release from G1 into S phase in 25 mM HU. A schematic representation of the 2D gel profiles observed in *RAD53* and *rad53* cells is shown. Histogram plots of the ratio between quantified "Spike" and "Large Y" intermediates signals are shown.

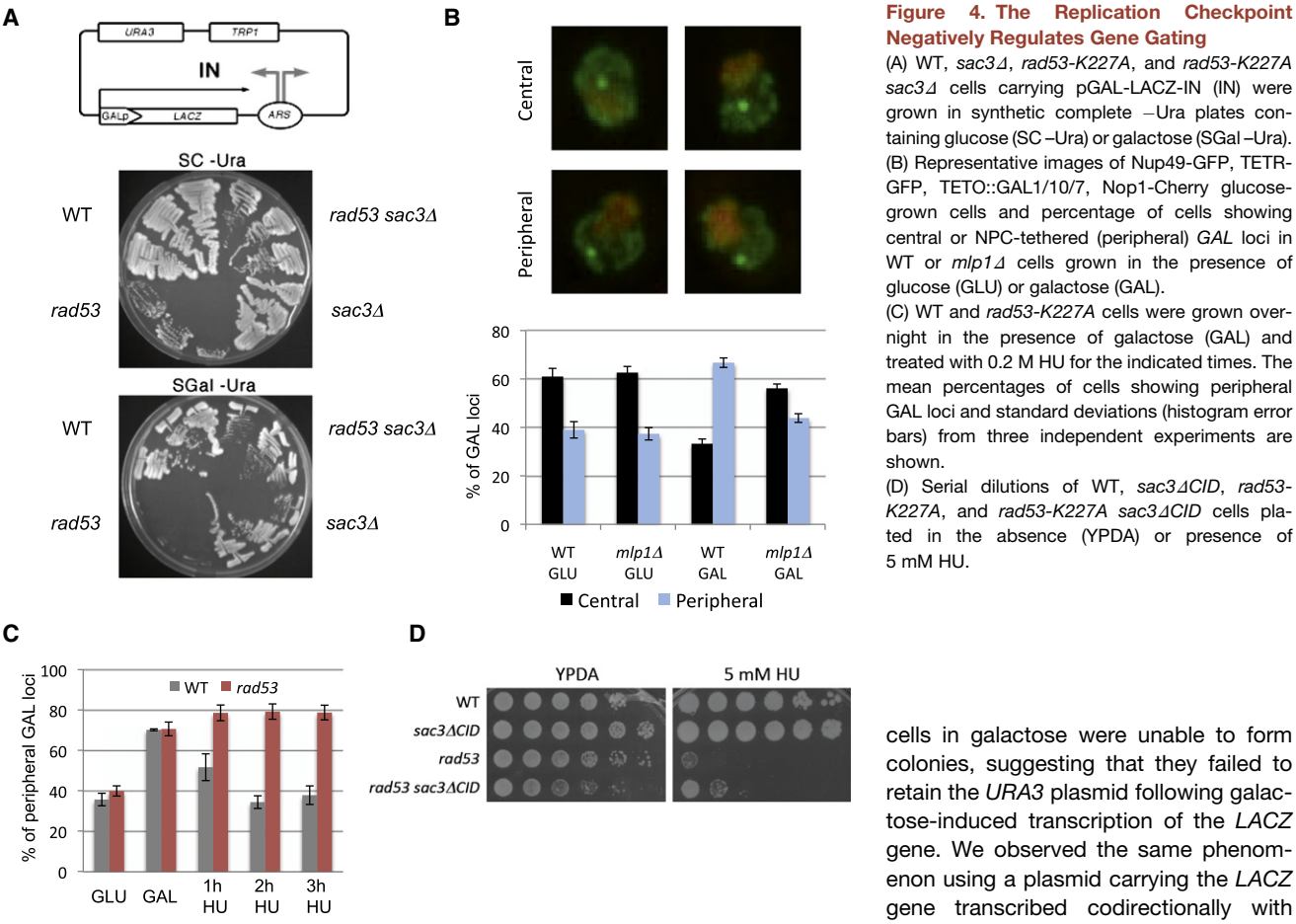

Figure 4. The Replication Checkpoint Negatively Regulates Gene Gating

(A) WT, *sac3Δ*, *rad53-K227A*, and *rad53-K227A sac3Δ* cells carrying pGAL-LACZ-IN (IN) were grown in synthetic complete −Ura plates containing glucose (SC –Ura) or galactose (SGal –Ura).

(B) Representative images of Nup49-GFP, TETR-GFP, TETO::GAL1/10/7, Nop1-Cherry glucose-grown cells and percentage of cells showing central or NPC-tethered (peripheral) *GAL* loci in WT or *mlp1Δ* cells grown in the presence of glucose (GLU) or galactose (GAL).

(C) WT and *rad53-K227A* cells were grown overnight in the presence of galactose (GAL) and treated with 0.2 M HU for the indicated times. The mean percentages of cells showing peripheral GAL loci and standard deviations (histogram error bars) from three independent experiments are shown.

(D) Serial dilutions of WT, *sac3ΔCID*, *rad53-K227A*, and *rad53-K227A sac3ΔCID* cells plated in the absence (YPDA) or presence of 5 mM HU.

of topological stress, as the association of DNA to a fixed nuclear structure would limit the rotation of helix strands around each other (Postow et al., 2001a, 2004). The consequent accumulation of positive supercoiling at transcribed genes might therefore provide the energy source to promote reversal of incoming forks, particularly in a checkpoint-defective genetic context that exhibits an altered replisome-fork association (Cobb et al., 2003; Lucca et al., 2004; Postow et al., 2001b). This hypothesis would have the following expectations: (1) part of the fork instability problems in *rad53* mutants should depend on transcription; (2) the Mec1-Rad53 checkpoint might control replicon integrity by releasing the topological barriers imposed by the coupling between mRNA synthesis and nuclear export; and (3) generating a physical discontinuity either at the level of the nuclear pore-bound TREX-2/THO complexes or in the DNA strands at the border between an incoming fork and a transcribed gene should relieve the topological stress causing fork reversal.

We tested the contribution of transcription on fork stability in *rad53* mutants. We transformed wild-type, *sac3*, *rad53*, and *rad53 sac3* cells with a plasmid carrying the *URA3*-selectable marker and a galactose-inducible *LACZ* gene that is transcribed head on with the left fork arising from *ARS209* (Figure 4A). Wild-type and *sac3* cells were able to stably retain the plasmid and grow in the absence of uracil with or without galactose. *rad53* cells in galactose were unable to form colonies, suggesting that they failed to retain the *URA3* plasmid following galactose-induced transcription of the *LACZ* gene. We observed the same phenomenon using a plasmid carrying the *LACZ* gene transcribed codirectionally with forks arising from *ARS209* (data not shown). We note that the *GAL1* promoter is leaky in the presence of glucose, thus explaining the growth defects of glucose-treated *rad53* cells. *SAC3* ablation was able to rescue the growth defects in glucose and the cell lethality in galactose owing to the *rad53* mutation. We conclude that the TREX-2 complex is detrimental for *rad53* viability when forks are destabilized by transcription, raising the possibility that, also in *rad53* mutants treated with low doses of HU (and therefore with an already compromised fork processivity), TREX-2 triggers fork abnormalities by tethering transcription with nuclear pore-mediated mRNA export.

We then tested whether Rad53 influences the nuclear envelope association of the transcribed *GAL* genes locus tagged with the TET operator/TETr-GFP system (Berger et al., 2008). We analyzed the percentage of cells exhibiting peripheral distribution of the GFP loci in logarithmically growing cells in the presence of glucose (repressing conditions for *GAL* genes) or galactose (Figure 4B). In glucose, the *GAL1/GAL10/GAL7* gene locus was localized to the nuclear periphery in 39% of the cells, whereas in galactose, in 67%. However, gene gating-defective *mlp1* mutants exhibited 37% and 44% peripheral foci in glucose and galactose, respectively, according to previous results (Brickner and Walter, 2004; Cabal et al., 2006; Tan-Wong et al., 2009). We then analyzed the localization of the *GAL* cluster in wild-type and *rad53* cells in the presence of HU and galactose

(Figure 4C). Whereas in wild-type cells, the percentage of peripheral GFP loci decreased, in *rad53*, it remained at high levels. Conversely, Rad53 did not affect GFP distribution in HU-treated cells in the presence of glucose (data not shown). We then interrupted in *rad53* cells the physical continuity within the TREX-2 complex by introducing the *sac3ΔCID* mutation that precludes the association with Sus1 and Cdc31 (Figure S1 available online) (Jani et al., 2009) and compared HU sensitivity and fork reversal in *rad53* and *rad53 sac3ΔCID* cells. The *sac3ΔCID* mutation rescued *rad53* HU sensitivity and fork reversal (Figure 4D) (data not shown).

Several NPC factors in the inner basket and some THO subunits are phosphorylated in a checkpoint-dependent manner in yeast and mammals, and in particular, Mpl1 is a Rad53 target (Figure 1C) (Chen et al., 2010; Matsuoka et al., 2007; Smolka et al., 2007). Ablation of *MLP1* in *rad53* cells prevented the peripheral localization of the *GAL* locus following HU treatment in galactose, resembling *mlp1* mutants (Figure 5A). In principle, Rad53 might counteract gene gating in S phase by negatively regulating NPC factors. The HU sensitivity of *rad53* cells might be ascribed to the inability to release the association between transcribed genes and the nuclear envelope and, in turn, to counteract the topological barriers arising when forks approach nuclear envelope-associated transcribed genes. We then ablated those NPC proteins exhibiting gene gating defects (Cabal et al., 2006; Tan-Wong et al., 2009) and tested their ability to alleviate *rad53* HU sensitivity. *NUP1* or *MLP1* deletions recapitulated the *rad53* suppression by TREX2 mutations (Figure 5B). Other proteins such as Nup2 and Nup60, which localize in the inner basket of the nuclear pore but do not physically interact with TREX-2 and whose role in gene gating is still controversial (Brickner et al., 2007; Cabal et al., 2006; Light et al., 2010), did not contribute to *rad53* HU sensitivity (Figure S2). Altogether, these results suggest that disrupting the association between the nuclear pore and TREX-2 proteins might alleviate the inability of *rad53* mutants to detach transcribed genes from the nuclear envelope. We then mutated serine 1710 in Mlp1 (Figure 5C) to an aspartic residue or an alanine to mimic constitutive Mlp1 phosphorylation or dephosphorylation, respectively. *mlp1-S1710D* counteracted nuclear peripheral localization of transcribed *GAL* genes, thus resembling loss-of-function *mlp1* mutations (Figure 5D). Conversely, *mlp1-S1710A* cells behaved like wild-type. Moreover, *mlp1-S1710D*, differently from *mlp1-S1710A*, also rescued *rad53* HU sensitivity (Figure 5E). These observations support the hypothesis that Rad53 inhibits gene gating though phosphorylation of Mlp1 and, possibly, other NPC proteins.

Fork Reversal Is Counteracted by Double-Strand Break Formation

We then explored the effect of releasing the topological tension within a region between a fork and a transcribed gene on fork reversal. We induced a DSB by overexpressing the HO endonuclease (Lee et al., 2000) that recognizes a specific site inserted between *ARS305* and the most proximal transcribed gene, *PDI1*, which causes fork pausing (Bermejo et al., 2009) and is bound by Top2, Hmo1, Hpr1, and Sac3 (Bermejo et al., 2009 and data not shown). In theory, the DSB-induced discontinuity in the helix strands should permit rotation of their free ends, thus leading to supercoiling relaxation and counteracting fork reversal.

We induced DSB formation and released the cells in the presence of HU (Figure 6). We analyzed the replication intermediates of *ARS305* and *ARS202*, an origin located on a different chromosome and not experiencing DSB formation. Strains bearing a noncleavable HO sequence were included as controls (HO-inc). Wild-type cells fired both origins, as indicated by the presence of large Y intermediates in *ARS305* and bubbles in *ARS202*, regardless of the presence or absence of the DSB (Doksani et al., 2009). *ARS202* fires later than *ARS305*, and bubbles can be detected at *ARS305* at earlier time points (data not shown). As expected, HU-treated HO-inc *rad53* cells fired both origins and accumulated X-shaped intermediates corresponding to reversed replication forks. DSB induction reduced reversed fork accumulation at *ARS305*, but not at the *ARS202* locus (Figure 6). We note that ~20% of the *AR305-PDI1* region remained uncut following HO induction, thus accounting for the residual Xs observed at *ARS305* in *rad53* cells. These observations suggest that, in vivo, positive supercoiling is a driving force for fork reversal in checkpoint mutants. Moreover, the findings that DSB formation mimics the effect of Sac3 ablation in preventing fork reversal within the same locus suggest that the integrity of the topological domain spanning the replisome and the nuclear pore-associated transcribed gene (Casolari et al., 2005) influences the fate of stalled forks and that Rad53, Top2, TREX-2, and THO complexes and NPC proteins collaborate in controlling the S phase architecture of transcribed loci to prevent aberrant transitions at replicating chromosomes.

DISCUSSION

Transcription is coordinated with replication to maintain genome integrity. Because fork advance and the progression of the transcription bubble generate positive supercoiling, a head-on collision between replication and transcription causes topological impediments and fork pausing (Liu and Alberts, 1995; Olavarrieta et al., 2002; Wang, 2002). Fork restart can occur through the displacement of the RNA polymerase complex (Pomerantz and O'Donnell, 2010). In vitro studies showed that codirectional collision between replication and transcription has little effects on fork progression (Liu and Alberts, 1995; Pomerantz and O'Donnell, 2008) unless the RNA polymerase stalls (Elías-Arnanz and Salas, 1997). There is evidence suggesting that the replisome can use mRNA as a primer after colliding codirectionally with RNA polymerase (Pomerantz and O'Donnell, 2008; Kogoma, 1997). Hence, it is not surprising that, in prokaryotes, which initiate DNA synthesis from a single origin, codirectional collision between forks and transcription bubbles is the preferred option (Brewer, 1988; Rocha, 2004). However, in multi-origin species, such as eukaryotes, transcription and replication collide both in head-on or codirectional ways. Indeed, transcribed genes always pause replication forks, regardless of their relative orientation (Azvolinsky et al., 2009; Bermejo et al., 2009), perhaps due to the Top2-mediated architecture of transcribed genes (Bermejo et al., 2009).

We show that the TREX-2-THO-dependent coupling of transcription, gene gating, and mRNA biogenesis causes aberrant

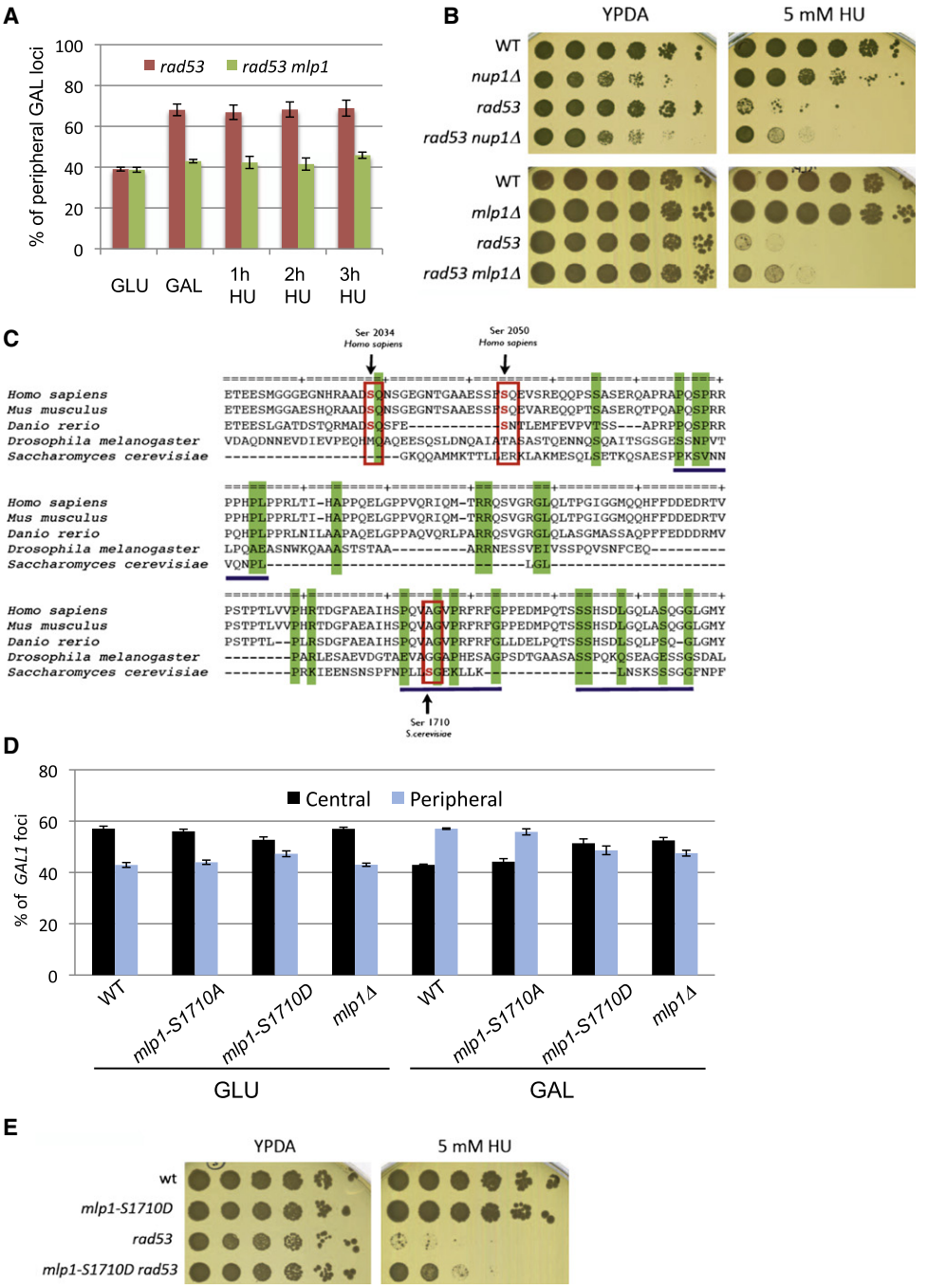

Figure 5. Nucleoporin Mutations Abolishing Gene Gating Suppress *rad53* Phenotypes

(A) *rad53-K227A* and *rad53-K227A mlp1Δ* cells were grown overnight with galactose (GAL) and treated with 0.2 M HU. The mean percentages of cells showing peripheral GAL loci and standard deviations (histogram error bars) from three independent experiments are shown.

(B) Serial dilutions of WT, *nup1Δ*, *rad53-K227A*, *rad53-K227A nup1Δ*, *mlp1Δ*, and *rad53-K227A mlp1Δ* cells plated in the absence (YPDA) or presence of 5 mM HU.

(C) Evolutionary comparison of a portion of the Mlp1 globular domain containing residues phosphorylated by checkpoint kinases. Conserved residues are labeled in green.

(D) Percentage of cells showing central or NPC-tethered (peripheral) *GAL* loci in WT, *mlp1S1710A*, *mlp1S1710D*, and *mlp1Δ* cells grown in the presence of glucose (GLU) or galactose (GAL).

(E) Serial dilutions of WT, *mlp1S1710D*, *rad53-K227A*, and *rad53-K227A mlp1S1710D* cells plated in the absence (YPDA) or presence of 5 mM HU.

For related data, see Figure S2.

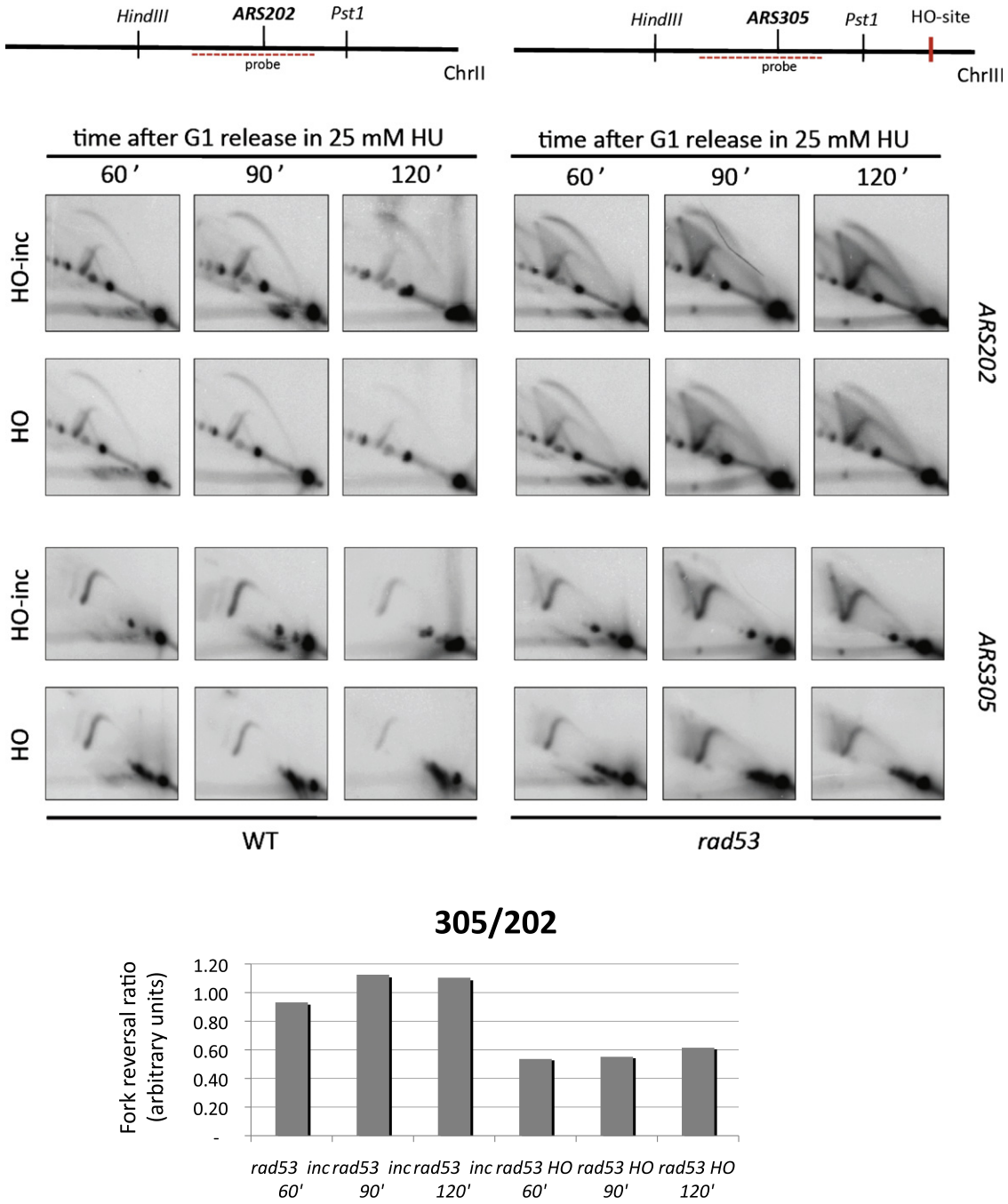

Figure 6. DSB Induction Counteracts Fork Reversal in *rad53* Mutants

Replication intermediates in WT HO-inc, WT HO, *rad53-K227A* HO-inc, and *rad53-K227A* HO cells following α factor-induced G1 arrest, DSB formation by galactose addition, and release in 25 mM HU. Schematic representations of the 2D gel digestion strategies used are shown. Histograms indicate the ratio between reversed fork signal intensities at *ARS305* and *ARS202* for *rad53* cells at each time point. For related data, see Figure S4.

transitions at stalled forks in checkpoint-defective cells. These observations, together with the findings that the genome-wide distribution of Hpr1 overlaps with that of RNA polymerase II and Top2 at transcribed genes (Bermejo et al., 2009), the checkpoint phosphorylates nuclear pore proteins (Chen et al., 2010; Smolka et al., 2007), Rad53 stoichiometrically associates with the Kap95 karyopherin (Smolka et al., 2005), and the relative distance between nuclear periphery and transcribed genes depends on the checkpoint, suggest that the physical continuity between transcribed genes and the nuclear envelope is modulated by the checkpoint to assist fork progression. The TREX-2 and THO-dependent topological impediments could, in part,

account for the genome-wide and nonpolar replication pausing at transcribed genes (Azvolinsky et al., 2009). It is tempting to speculate that, whereas eukaryotes have evolved the checkpoint response to relieve the topological tension that occurs from the nuclear envelope-mediated mRNA export process, prokaryotes, deprived of the nuclear envelope, have evolved codirectionality between replication forks and transcription to avoid topological stress. And perhaps, the lack of transcription during the embryonic cell cycle is the reason that embryonic chromosome replication is not assisted by the checkpoint response, which is, in fact, established as soon as the cell enters the somatic cell cycle and transcription begins.

TREX-2-THO mutants exhibit slow replication and HU sensitivity and accumulate checkpoint signals under unperturbed conditions (Gómez-González et al., 2009; González-Aguilera et al., 2008; Wellinger et al., 2006). This apparent paradox can be explained by the pathological accumulation of R loops (Wellinger et al., 2006), and in fact, these phenotypes are alleviated by RNase H overexpression (Huertas and Aguilera, 2003). The replication problems and HU sensitivity of TREX-2-THO mutants can also account for the inability of TREX-2-THO ablation to suppress *rad53* lethality at higher HU concentrations.

The topology within a transcription loop that faces a collision with an approaching replication fork might be challenging (Figure 7A). The coupling between RNA synthesis and export implies that, as the RNA polymerase rotates along the DNA duplex, the 5′ terminus of the RNA molecule is engaged by the export machinery anchored to the nuclear pore. This will impose torsional stress and entangle the mRNA within the loop. The incoming fork is expected to further enhance the topological complexity. We speculate that Top2 might reduce the topological tension, perhaps with the contribution of Hpr1 that shares homology with type I topoisomerases (Aguilera and Klein, 1990; Wang et al., 1990). Interestingly, Top2 and Hmo1 physically interact with Yra1 (Figure S1) (Ho et al., 2002; Krogan et al., 2006), and *top2* mutants are synthetic sick with *HPR1* or *SAC3* mutations (data not shown) (Aguilera and Klein, 1990). Based on our observations on HU-induced fork stress, we speculate (Figures 7A and 7B) that passage across transcribed units might depend on the regulation of the gene gating apparatus to allow rotation of the unreplicated region and unfolding of the transcriptional domain. This regulatory process is likely specific for RNA Pol II-transcribed genes. Replication pausing also occurs at tRNA genes. Intriguingly, Mec1 and Rad53 repress tRNA transcription (Nguyen et al., 2010) and inhibit tRNA nuclear export via relocalization of the Los1 karyopherin (Ghavidel et al., 2007), which interacts with the checkpoint targets Nup2 and Nsp1 (Hellmuth et al., 1998) (Figure S3A). Fork progression through pausing elements requires optimal dNTP pools. Mec1, Rad53, and Dun1 influence dNTP pools by regulating the transcription of RNR genes (Allen et al., 1994), the stability of the RNR inhibitor Sml1 (Zhao and Rothstein, 2002), and the nuclear localization of RNR through Wtm1 and Wtm2 (Lee and Elledge, 2006), which interact with the Nup60 and Srp1 nucleoporins (Decourty et al., 2008) (Figure S3A). We propose that the Mec1 checkpoint protects fork integrity at transcription-dependent pausing sites by phosphorylating nuclear pore factors in order to simultaneously regulate gene gating at Pol II-transcribed genes, tRNA nuclear export, and RNR activity. Intriguingly, the Serine 1710 (Figure 5C) of Mlp1 localizes within a highly conserved globular domain of the protein that mediates the interaction between Mlp1 and the Nab2 RNA-binding protein. Moreover, in metazoa, two Mlp1 residues for ATR-dependent phosphorylation map within the same globular domain. The scenario described above is also consistent with the Rad53 interaction network (Figure S3A). How Mec1/ATR sense fork pausing at transcribed regions under physiological conditions needs to be addressed. It is possible that short ssDNA tracts may accumulate when forks pause at transcribed regions, thus promoting a local activation of Mec1. However, we cannot rule out that Mec1/ATR monitor mechanical vibrations caused by the topological tension when forks encounter gated genes. It is intriguing to note that PI3 kinases, including Mec1/ATR and Tel1/ATM, and the Rad53-interacting importin-β Srp1 and Kap95 contain HEAT domain (Conti and Rhodes, 2009; Perry and Kleckner, 2003) elastic connectors, ideal for monitoring mechanical stress (Grinthal et al., 2010).

Nuclear pores have been implicated in coordinating DNA repair to SUMO-dependent ubiquitylation processes (Nagai et al., 2008) and preventing recombination events (Loeillet et al., 2005). We show that the nuclear pore apparatus also influences the stability of forks encountering gated genes. This is also supported by evidence connecting replication proteins to NPCs (Figure S3B). mRNA export is coupled to transcription and splicing in metazoa (Köhler and Hurt, 2007). It would not be surprising that the physical tethering of mRNAs to the splicing apparatus might also influence chromosome topology in higher eukaryotes. Intriguingly, a recent genome-wide screen has unmasked mRNA processing factors as mediators of genome stability (Paulsen et al., 2009).

Our data imply that the S phase architecture of transcribed units is coordinated with fork progression to prevent topological impediments causing fork reversal (Figure 7B). Three independent findings support this view: (1) fork reversal can be counteracted by resolving the local topological complexity through DSB formation; (2) reversed forks accumulate following CPT treatment (A. Ray Chaudhuri and M. Lopes, personal communication) that freezes Top1-DNA abducts in front of the fork (Koster et al., 2007); and (3) cruciform structures accumulate at forks even in checkpoint-proficient cells following genetic inactivation of Top1 and Top2 (Figure S4). In this scenario, those pathological conditions leading to either deregulated S phase transcription and/or increasing the number of forks may enhance topological impediments and therefore the potentiality for fork reversal. This is the case in a checkpoint-defective context in which, on top of the inability to detach the genome association with the nuclear envelope, the unscheduled firing of dormant origins increases the number of forks that might undergo reversal. Accordingly, CHK1-deficient cells exhibit increased origin activation and reduced rates of fork progression that can be alleviated by counteracting origin firing though Cdk2 or Cdc7 inhibition (Petermann et al., 2010).

Our findings have relevant implications for cancer. Besides the well-established notion of the checkpoint response acting as an anticancer barrier (Halazonetis et al., 2008), we note that the human Mlp1 ortholog TPR is translocated in different cancers (Köhler and Hurt, 2010). Finally, the mechanisms described

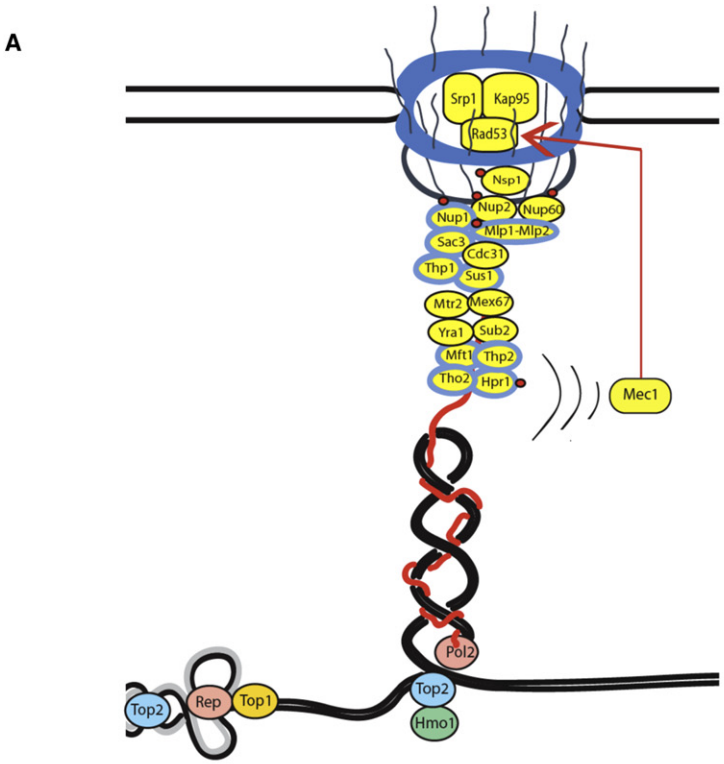

Figure 7. Hypothetical Transitions at Forks Encountering Nuclear Pore Gated Genes

(A) Hypothetical schematic representation of the topological architecture of forks encountering nuclear pore-gated transcribed genes. Small red circles represent phosphorylation events mediated by the checkpoint. Yellow ovals surrounded by blue indicate those proteins whose gene deletions rescue *rad53*. The red line indicates mRNA. We speculate that Mec1 senses vibrations resulting from the clash between forks and gated genes. Rad53 is then activated and phosphorylates nucleoporins in the inner basket. Some of these phosphorylation events might also regulate tRNA metabolism and/or dNTP pools. See text for details.

(B) The "R" indicates replisome; "P," RNA polymerase II. In WT cells, forks pause in front of the transcribed region (Azvolinsky et al., 2009) and activate the checkpoint (DDR). Checkpoint activation then releases the tethering between the transcribed gene and the nuclear pore. Consequently, the architectural domain of the transcribed region (Bermejo et al., 2009) is simplified, thus enabling fork restart. In *rad53* mutants, the clash between the fork and the transcribed region is not assisted by the checkpoint, and consequently, the fork collapses, leading to replisome dissociation and fork reversal owing to the unsolved topological stress.

For related information, see Figure S3.

above might also be relevant for oncogene-induced replication stress, considering that the oncogenic stimuli cause massive transcription deregulation.

EXPERIMENTAL PROCEDURES

S. cerevisiae Strains

Strains are listed in Table S1. *sac3ΔCID*, *mlp1S1710A*, and *mlp1S1710D* mutants were constructed by *delitto perfetto* (Storici and Resnick, 2006). pGW-RNH1 plasmid was a gift from R. Crouch. pGAL-LACZ-IN plasmid was constructed by amplifying GAL1-LacZ-CYCt from pRS416GAL1LacZ (Chávez and Aguilera, 1997) and subcloning into pFERNU-3 (Prado and Aguilera, 2005).

Synthetic Genetic Array Screening

Synthetic genetic arrays (SGA) and generation of a GAL1-*rad53-D339A* double-mutant collection was carried out as described (Lopes et al., 2001; Tong et al., 2001). *rad53-D339A* HU sensitivity suppressors were isolated by comparing growth of double mutants replicated on galactose or glucose plates containing 10 mM HU.

Gene Gating Analysis by Fluorescence Microscopy

Localization of the *GAL* locus was scored by spinning disk confocal microscope as described (Berger et al., 2008). Cells were fixed in 4% formaldehyde, placed on a 28 mm diameter coverslip mounted in an Okolab metal ring chamber, and covered with a thin slice of H_2O agar 1%. Z stack series (0.2 micron step) were obtained with an UltraVIEW VoX (Perkin Elmer) spinning disk confocal microscope using a 100× oil-immersion objective (NA = 1.49) using 488 nm

and 561 nm laser wavelengths for GFP and Cherry signal detection, respectively. Image analysis was performed using ImageJ 1.43u (http://rsb.info.nih.gov/ij) software on the maximum projection of every Z stack.

BrdU-IP Chip Analysis

S. cerevisiae oligonucleotide microarrays were provided by Affymetrix. The BrdU-IP chip analysis was carried out as described (Fachinetti et al., 2010; Katou et al., 2003), employing anti-BrdU antibody (MBL M1-11-3).

Two-Dimensional Gel Analysis of Replication Intermediates

In vivo psoralen crosslinking and 2D gel analysis have been described (Brewer and Fangman, 1987; Lopes et al., 2003). PstI/EcoRI digestions were used unless otherwise stated. Induction of a HO-mediated DSB close to the *ARS305* origin has been described (Doksani et al., 2009).

ACCESSION NUMBERS

Experimental data are available on the Gene Expression Omnibus database with accession number GSE30024.

SUPPLEMENTAL INFORMATION

Supplemental Information includes four figures and one table and can be found with this article online at doi:10.1016/j.cell.2011.06.033.

ACKNOWLEDGMENTS

We thank Markus Smolka, Nancy Kleckner, Ed Hurt, Massimo Lopes, Giordano Liberi, Dana Branzei, and all members of our laboratories for discussions and Robert Crouch, Francesca Storici, Arta Ajazi, Giulia Bastianello, Dario Parazzoli, Amanda Oldani, and Maria Garcia-Rubio for reagents, advice, and technical support. M.F. was supported by grants from FIRC, AIRC, AICR, Telethon-Italy, E.U. GENICA-project, and Italian Ministry of Health. A.A. was supported by the Spanish Ministry of Science and Innovation (grants BFU2006-05260 and Consolider Ingenio 2010 CSD2007-0015); H.K. by NIH grant GM053738; and R.B. by a UICC Yamagiwa-Yoshida Memorial International Cancer Study. T.C. and A.C. were supported by FIRC fellowships.

Received: January 2, 2011
Revised: April 22, 2011
Accepted: June 15, 2011
Published: July 21, 2011

REFERENCES

Aguilera, A. (2005). Cotranscriptional mRNP assembly: from the DNA to the nuclear pore. Curr. Opin. Cell Biol. *17*, 242–250.

Aguilera, A., and Klein, H.L. (1990). HPR1, a novel yeast gene that prevents intrachromosomal excision recombination, shows carboxy-terminal homology to the Saccharomyces cerevisiae TOP1 gene. Mol. Cell. Biol. *10*, 1439–1451.

Allen, J.B., Zhou, Z., Siede, W., Friedberg, E.C., and Elledge, S.J. (1994). The SAD1/RAD53 protein kinase controls multiple checkpoints and DNA damage-induced transcription in yeast. Genes Dev. *8*, 2401–2415.

Azvolinsky, A., Giresi, P.G., Lieb, J.D., and Zakian, V.A. (2009). Highly transcribed RNA polymerase II genes are impediments to replication fork progression in Saccharomyces cerevisiae. Mol. Cell *34*, 722–734.

Berger, A.B., Cabal, G.G., Fabre, E., Duong, T., Buc, H., Nehrbass, U., Olivo-Marin, J.C., Gadal, O., and Zimmer, C. (2008). High-resolution statistical mapping reveals gene territories in live yeast. Nat. Methods *5*, 1031–1037.

Bermejo, R., Branzei, D., and Foiani, M. (2008). Cohesion by topology: sister chromatids interlocked by DNA. Genes Dev. *22*, 2297–2301.

Bermejo, R., Capra, T., Gonzalez-Huici, V., Fachinetti, D., Cocito, A., Natoli, G., Katou, Y., Mori, H., Kurokawa, K., Shirahige, K., and Foiani, M. (2009). Genome-organizing factors Top2 and Hmo1 prevent chromosome fragility at sites of S phase transcription. Cell *138*, 870–884.

Branzei, D., and Foiani, M. (2010). Maintaining genome stability at the replication fork. Nat. Rev. Mol. Cell Biol. *11*, 208–219.

Brewer, B.J. (1988). When polymerases collide: replication and the transcriptional organization of the E. coli chromosome. Cell *53*, 679–686.

Brewer, B.J., and Fangman, W.L. (1987). The localization of replication origins on ARS plasmids in S. cerevisiae. Cell *51*, 463–471.

Brickner, J.H., and Walter, P. (2004). Gene recruitment of the activated INO1 locus to the nuclear membrane. PLoS Biol. *2*, e342.

Brickner, D.G., Cajigas, I., Fondufe-Mittendorf, Y., Ahmed, S., Lee, P.C., Widom, J., and Brickner, J.H. (2007). H2A.Z-mediated localization of genes at the nuclear periphery confers epigenetic memory of previous transcriptional state. PLoS Biol. *5*, e81.

Cabal, G.G., Genovesio, A., Rodriguez-Navarro, S., Zimmer, C., Gadal, O., Lesne, A., Buc, H., Feuerbach-Fournier, F., Olivo-Marin, J.C., Hurt, E.C., and Nehrbass, U. (2006). SAGA interacting factors confine sub-diffusion of transcribed genes to the nuclear envelope. Nature *441*, 770–773.

Casolari, J.M., Brown, C.R., Drubin, D.A., Rando, O.J., and Silver, P.A. (2005). Developmentally induced changes in transcriptional program alter spatial organization across chromosomes. Genes Dev. *19*, 1188–1198.

Chávez, S., and Aguilera, A. (1997). The yeast HPR1 gene has a functional role in transcriptional elongation that uncovers a novel source of genome instability. Genes Dev. *11*, 3459–3470.

Chen, S.H., Albuquerque, C.P., Liang, J., Suhandynata, R.T., and Zhou, H. (2010). A proteome-wide analysis of kinase-substrate network in the DNA damage response. J. Biol. Chem. *285*, 12803–12812.

Cobb, J.A., Bjergbaek, L., Shimada, K., Frei, C., and Gasser, S.M. (2003). DNA polymerase stabilization at stalled replication forks requires Mec1 and the RecQ helicase Sgs1. EMBO J. *22*, 4325–4336.

Conti, E., and Rhodes, D. (2009). Modern times: not for the faint-hearted. Curr. Opin. Struct. Biol. *19*, 62–64.

Cotta-Ramusino, C., Fachinetti, D., Lucca, C., Doksani, Y., Lopes, M., Sogo, J., and Foiani, M. (2005). Exo1 processes stalled replication forks and counteracts fork reversal in checkpoint-defective cells. Mol. Cell *17*, 153–159.

Decourty, L., Saveanu, C., Zemam, K., Hantraye, F., Frachon, E., Rousselle, J.C., Fromont-Racine, M., and Jacquier, A. (2008). Linking functionally related genes by sensitive and quantitative characterization of genetic interaction profiles. Proc. Natl. Acad. Sci. USA *105*, 5821–5826.

Doksani, Y., Bermejo, R., Fiorani, S., Haber, J.E., and Foiani, M. (2009). Replicon dynamics, dormant origin firing, and terminal fork integrity after double-strand break formation. Cell *137*, 247–258.

Drubin, D.A., Garakani, A.M., and Silver, P.A. (2006). Motion as a phenotype: the use of live-cell imaging and machine visual screening to characterize transcription-dependent chromosome dynamics. BMC Cell Biol. *7*, 19.

Elías-Arnanz, M., and Salas, M. (1997). Bacteriophage phi29 DNA replication arrest caused by codirectional collisions with the transcription machinery. EMBO J. *16*, 5775–5783.

Fachinetti, D., Bermejo, R., Cocito, A., Minardi, S., Katou, Y., Kanoh, Y., Shirahige, K., Azvolinsky, A., Zakian, V.A., and Foiani, M. (2010). Replication termination at eukaryotic chromosomes is mediated by Top2 and occurs at genomic loci containing pausing elements. Mol. Cell *39*, 595–605.

Fay, D.S., Sun, Z., and Stern, D.F. (1997). Mutations in SPK1/RAD53 that specifically abolish checkpoint but not growth-related functions. Curr. Genet. *31*, 97–105.

Feng, W., Collingwood, D., Boeck, M.E., Fox, L.A., Alvino, G.M., Fangman, W.L., Raghuraman, M.K., and Brewer, B.J. (2006). Genomic mapping of single-stranded DNA in hydroxyurea-challenged yeasts identifies origins of replication. Nat. Cell Biol. *8*, 148–155.

Ghavidel, A., Kislinger, T., Pogoutse, O., Sopko, R., Jurisica, I., and Emili, A. (2007). Impaired tRNA nuclear export links DNA damage and cell-cycle checkpoint. Cell *131*, 915–926.

Gómez-González, B., García-Rubio, M., Bermejo, R., Gaillard, H., Shirahige, K., Marín, A., Foiani, M., and Aguilera, A. (2011). Genome-wide function of

THO/TREX in active genes prevents R-loop-dependent replication obstacles. EMBO J. Published online June 24, 2011. 10.1038/emboj.2011.206.

Gómez-González, B., Felipe-Abrio, I., and Aguilera, A. (2009). The S-phase checkpoint is required to respond to R-loops accumulated in THO mutants. Mol. Cell. Biol. *29*, 5203–5213.

González-Aguilera, C., Tous, C., Gómez-González, B., Huertas, P., Luna, R., and Aguilera, A. (2008). The THP1-SAC3-SUS1-CDC31 complex works in transcription elongation-mRNA export preventing RNA-mediated genome instability. Mol. Biol. Cell *19*, 4310–4318.

Grinthal, A., Adamovic, I., Weiner, B., Karplus, M., and Kleckner, N. (2010). PR65, the HEAT-repeat scaffold of phosphatase PP2A, is an elastic connector that links force and catalysis. Proc. Natl. Acad. Sci. USA *107*, 2467–2472.

Halazonetis, T.D., Gorgoulis, V.G., and Bartek, J. (2008). An oncogene-induced DNA damage model for cancer development. Science *319*, 1352–1355.

Hellmuth, K., Lau, D.M., Bischoff, F.R., Künzler, M., Hurt, E., and Simos, G. (1998). Yeast Los1p has properties of an exportin-like nucleocytoplasmic transport factor for tRNA. Mol. Cell. Biol. *18*, 6374–6386.

Ho, Y., Gruhler, A., Heilbut, A., Bader, G.D., Moore, L., Adams, S.L., Millar, A., Taylor, P., Bennett, K., Boutilier, K., et al. (2002). Systematic identification of protein complexes in Saccharomyces cerevisiae by mass spectrometry. Nature *415*, 180–183.

Huertas, P., and Aguilera, A. (2003). Cotranscriptionally formed DNA:RNA hybrids mediate transcription elongation impairment and transcription-associated recombination. Mol. Cell *12*, 711–721.

Jani, D., Lutz, S., Marshall, N.J., Fischer, T., Köhler, A., Ellisdon, A.M., Hurt, E., and Stewart, M. (2009). Sus1, Cdc31, and the Sac3 CID region form a conserved interaction platform that promotes nuclear pore association and mRNA export. Mol. Cell *33*, 727–737.

Katou, Y., Kanoh, Y., Bando, M., Noguchi, H., Tanaka, H., Ashikari, T., Sugimoto, K., and Shirahige, K. (2003). S-phase checkpoint proteins Tof1 and Mrc1 form a stable replication-pausing complex. Nature *424*, 1078–1083.

Kogoma, T. (1997). Stable DNA replication: interplay between DNA replication, homologous recombination, and transcription. Microbiol. Mol. Biol. Rev. *61*, 212–238.

Köhler, A., and Hurt, E. (2007). Exporting RNA from the nucleus to the cytoplasm. Nat. Rev. Mol. Cell Biol. *8*, 761–773.

Köhler, A., and Hurt, E. (2010). Gene regulation by nucleoporins and links to cancer. Mol. Cell *38*, 6–15.

Koster, D.A., Palle, K., Bot, E.S., Bjornsti, M.A., and Dekker, N.H. (2007). Antitumour drugs impede DNA uncoiling by topoisomerase I. Nature *448*, 213–217.

Krogan, N.J., Cagney, G., Yu, H., Zhong, G., Guo, X., Ignatchenko, A., Li, J., Pu, S., Datta, N., Tikuisis, A.P., et al. (2006). Global landscape of protein complexes in the yeast Saccharomyces cerevisiae. Nature *440*, 637–643.

Lee, Y.D., and Elledge, S.J. (2006). Control of ribonucleotide reductase localization through an anchoring mechanism involving Wtm1. Genes Dev. *20*, 334–344.

Lee, S.E., Pellicioli, A., Demeter, J., Vaze, M.P., Gasch, A.P., Malkova, A., Brown, P.O., Botstein, D., Stearns, T., Foiani, M., and Haber, J.E. (2000). Arrest, adaptation, and recovery following a chromosome double-strand break in Saccharomyces cerevisiae. Cold Spring Harb. Symp. Quant. Biol. *65*, 303–314.

Light, W.H., Brickner, D.G., Brand, V.R., and Brickner, J.H. (2010). Interaction of a DNA zip code with the nuclear pore complex promotes H2A.Z incorporation and INO1 transcriptional memory. Mol. Cell *40*, 112–125.

Liu, B., and Alberts, B.M. (1995). Head-on collision between a DNA replication apparatus and RNA polymerase transcription complex. Science *267*, 1131–1137.

Loeillet, S., Palancade, B., Cartron, M., Thierry, A., Richard, G.F., Dujon, B., Doye, V., and Nicolas, A. (2005). Genetic network interactions among replication, repair and nuclear pore deficiencies in yeast. DNA Repair (Amst.) *4*, 459–468.

Lopes, M., Cotta-Ramusino, C., Pellicioli, A., Liberi, G., Plevani, P., Muzi-Falconi, M., Newlon, C.S., and Foiani, M. (2001). The DNA replication checkpoint response stabilizes stalled replication forks. Nature *412*, 557–561.

Lopes, M., Cotta-Ramusino, C., Liberi, G., and Foiani, M. (2003). Branch migrating sister chromatid junctions form at replication origins through Rad51/Rad52-independent mechanisms. Mol. Cell *12*, 1499–1510.

Lucca, C., Vanoli, F., Cotta-Ramusino, C., Pellicioli, A., Liberi, G., Haber, J., and Foiani, M. (2004). Checkpoint-mediated control of replisome-fork association and signalling in response to replication pausing. Oncogene *23*, 1206–1213.

Luna, R., Gaillard, H., González-Aguilera, C., and Aguilera, A. (2008). Biogenesis of mRNPs: integrating different processes in the eukaryotic nucleus. Chromosoma *117*, 319–331.

Matsuoka, S., Ballif, B.A., Smogorzewska, A., McDonald, E.R., 3rd, Hurov, K.E., Luo, J., Bakalarski, C.E., Zhao, Z., Solimini, N., Lerenthal, Y., et al. (2007). ATM and ATR substrate analysis reveals extensive protein networks responsive to DNA damage. Science *316*, 1160–1166.

Nagai, S., Dubrana, K., Tsai-Pflugfelder, M., Davidson, M.B., Roberts, T.M., Brown, G.W., Varela, E., Hediger, F., Gasser, S.M., and Krogan, N.J. (2008). Functional targeting of DNA damage to a nuclear pore-associated SUMO-dependent ubiquitin ligase. Science *322*, 597–602.

Newlon, C.S., Collins, I., Dershowitz, A., Deshpande, A.M., Greenfeder, S.A., Ong, L.Y., and Theis, J.F. (1993). Analysis of replication origin function on chromosome III of Saccharomyces cerevisiae. Cold Spring Harb. Symp. Quant. Biol. *58*, 415–423.

Nguyen, V.C., Clelland, B.W., Hockman, D.J., Kujat-Choy, S.L., Mewhort, H.E., and Schultz, M.C. (2010). Replication stress checkpoint signaling controls tRNA gene transcription. Nat. Struct. Mol. Biol. *17*, 976–981.

Olavarrieta, L., Hernández, P., Krimer, D.B., and Schvartzman, J.B. (2002). DNA knotting caused by head-on collision of transcription and replication. J. Mol. Biol. *322*, 1–6.

Paulsen, R.D., Soni, D.V., Wollman, R., Hahn, A.T., Yee, M.C., Guan, A., Hesley, J.A., Miller, S.C., Cromwell, E.F., Solow-Cordero, D.E., et al. (2009). A genome-wide siRNA screen reveals diverse cellular processes and pathways that mediate genome stability. Mol. Cell *35*, 228–239.

Perry, J., and Kleckner, N. (2003). The ATRs, ATMs, and TORs are giant HEAT repeat proteins. Cell *112*, 151–155.

Petermann, E., Woodcock, M., and Helleday, T. (2010). Chk1 promotes replication fork progression by controlling replication initiation. Proc. Natl. Acad. Sci. USA *107*, 16090–16095.

Poloumienko, A., Dershowitz, A., De, J., and Newlon, C.S. (2001). Completion of replication map of Saccharomyces cerevisiae chromosome III. Mol. Biol. Cell *12*, 3317–3327.

Pomerantz, R.T., and O'Donnell, M. (2008). The replisome uses mRNA as a primer after colliding with RNA polymerase. Nature *456*, 762–766.

Pomerantz, R.T., and O'Donnell, M. (2010). Direct restart of a replication fork stalled by a head-on RNA polymerase. Science *327*, 590–592.

Postow, L., Crisona, N.J., Peter, B.J., Hardy, C.D., and Cozzarelli, N.R. (2001a). Topological challenges to DNA replication: conformations at the fork. Proc. Natl. Acad. Sci. USA *98*, 8219–8226.

Postow, L., Ullsperger, C., Keller, R.W., Bustamante, C., Vologodskii, A.V., and Cozzarelli, N.R. (2001b). Positive torsional strain causes the formation of a four-way junction at replication forks. J. Biol. Chem. *276*, 2790–2796.

Postow, L., Hardy, C.D., Arsuaga, J., and Cozzarelli, N.R. (2004). Topological domain structure of the Escherichia coli chromosome. Genes Dev. *18*, 1766–1779.

Prado, F., and Aguilera, A. (2005). Impairment of replication fork progression mediates RNA polII transcription-associated recombination. EMBO J. *24*, 1267–1276.

Rocha, E.P. (2004). The replication-related organization of bacterial genomes. Microbiology *150*, 1609–1627.

Rougemaille, M., Dieppois, G., Kisseleva-Romanova, E., Gudipati, R.K., Lemoine, S., Blugeon, C., Boulay, J., Jensen, T.H., Stutz, F., Devaux, F., and Libri, D. (2008). THO/Sub2p functions to coordinate 3′-end processing with gene-nuclear pore association. Cell *135*, 308–321.

Santocanale, C., and Diffley, J.F. (1998). A Mec1- and Rad53-dependent checkpoint controls late-firing origins of DNA replication. Nature *395*, 615–618.

Schvartzman, J.B., and Stasiak, A. (2004). A topological view of the replicon. EMBO Rep. *5*, 256–261.

Segurado, M., and Diffley, J.F. (2008). Separate roles for the DNA damage checkpoint protein kinases in stabilizing DNA replication forks. Genes Dev. *22*, 1816–1827.

Shirahige, K., Hori, Y., Shiraishi, K., Yamashita, M., Takahashi, K., Obuse, C., Tsurimoto, T., and Yoshikawa, H. (1998). Regulation of DNA-replication origins during cell-cycle progression. Nature *395*, 618–621.

Smolka, M.B., Albuquerque, C.P., Chen, S.H., Schmidt, K.H., Wei, X.X., Kolodner, R.D., and Zhou, H. (2005). Dynamic changes in protein-protein interaction and protein phosphorylation probed with amine-reactive isotope tag. Mol. Cell. Proteomics *4*, 1358–1369.

Smolka, M.B., Albuquerque, C.P., Chen, S.H., and Zhou, H. (2007). Proteome-wide identification of in vivo targets of DNA damage checkpoint kinases. Proc. Natl. Acad. Sci. USA *104*, 10364–10369.

Sogo, J.M., Lopes, M., and Foiani, M. (2002). Fork reversal and ssDNA accumulation at stalled replication forks owing to checkpoint defects. Science *297*, 599–602.

Storici, F., and Resnick, M.A. (2006). The delitto perfetto approach to in vivo site-directed mutagenesis and chromosome rearrangements with synthetic oligonucleotides in yeast. Methods Enzymol. *409*, 329–345.

Tan-Wong, S.M., Wijayatilake, H.D., and Proudfoot, N.J. (2009). Gene loops function to maintain transcriptional memory through interaction with the nuclear pore complex. Genes Dev. *23*, 2610–2624.

Thomas, B.J., and Rothstein, R. (1989). Elevated recombination rates in transcriptionally active DNA. Cell *56*, 619–630.

Tong, A.H., Evangelista, M., Parsons, A.B., Xu, H., Bader, G.D., Pagé, N., Robinson, M., Raghibizadeh, S., Hogue, C.W., Bussey, H., et al. (2001). Systematic genetic analysis with ordered arrays of yeast deletion mutants. Science *294*, 2364–2368.

Wang, J.C. (2002). Cellular roles of DNA topoisomerases: a molecular perspective. Nat. Rev. Mol. Cell Biol. *3*, 430–440.

Wang, J.C., Caron, P.R., and Kim, R.A. (1990). The role of DNA topoisomerases in recombination and genome stability: a double-edged sword? Cell *62*, 403–406.

Wellinger, R.E., Prado, F., and Aguilera, A. (2006). Replication fork progression is impaired by transcription in hyperrecombinant yeast cells lacking a functional THO complex. Mol. Cell. Biol. *26*, 3327–3334.

Zhao, X., and Rothstein, R. (2002). The Dun1 checkpoint kinase phosphorylates and regulates the ribonucleotide reductase inhibitor Sml1. Proc. Natl. Acad. Sci. USA *99*, 3746–3751.

Zheng, P., Fay, D.S., Burton, J., Xiao, H., Pinkham, J.L., and Stern, D.F. (1993). SPK1 is an essential S-phase-specific gene of Saccharomyces cerevisiae that encodes a nuclear serine/threonine/tyrosine kinase. Mol. Cell. Biol. *13*, 5829–5842.

Zou, L., and Elledge, S.J. (2003). Sensing DNA damage through ATRIP recognition of RPA-ssDNA complexes. Science *300*, 1542–1548.